UNIVERSITY OF MICHIGAN

DEPARTMENT OF MECHANICAL ENGINEERING
CAVITATION AND MULTIPHASE FLOW LABORATORY

Report No. UMICH 014456-3-I

# PREDICTIVE CAPABILITY FOR CAVITATION DAMAGE FROM BUBBLE COLLAPSE PULSE COUNT SPECTRA

(Submitted I.Mech.E. conference "Scaling for Performance Prediction in Rotodynamic Machines", 6-8 Sept, 1977, University of Stirling, U.K.)

by

F. G. Hammitt
S. A. Barber
M. K. De
A. N. El Hasrouni

Financial support provided by: Office of Naval Research
Contract No. NOOO14-76-C-0697.

November, 1976

ABSTRACT

The concept of "cavitation erosion efficiency, $\eta_{cav}$ is advanced and defined, relating acoustic power in the cavitation field to erosion power, i.e., the product of volume loss rate and material failure energy, here considered to be "ultimate resilience". The relative constancy of $\eta_{cav}$ is confirmed for damage tests in both sodium and water over a range of pressure and temperature in a vibratory facility. Good correlation between bubble collapse pulse count spectrum area, i.e., "acoustic power", and measured volume loss rate is shown. Thus the possibility of à priori prediction of eventual erosion rate from such pulse count measurements is confirmed.

A direct comparison of sodium and water results shows their damaging capabilities to be of comparable magnitude, with sodium $\sim$2.5 x more damaging.

Application of these vibratory facility damage and acoustic results to flowing systems is discussed.

## I. Introduction

One of the major present day difficulties facing designers of liquid-flow machinery components where cavitation is a possibility, is the present almost complete inability to predict possible cavitation damage rates, or even their probable existence, in field machines from laboratory tests which are both feasible and practical. Hence there often exists the necessity for very expensive and time-consuming long-term cavitation damage tests in near prototype-scale machines. This is especially a problem in nuclear reactor circulating pumps, particularly for the sodium-cooled fast breeder reactor concepts. Such long-term damage tests at one-half scale were in fact recently performed for the SNR-300 reactor pumps (1,2, eg.). It is the primary purpose of the University of Michigan research here described to develop a technique for the prediction of such eventual long-term cavitation damage rates, at least to a degree of engineering utility, from feasible and relatively modest laboratory tests. It is hoped to attain this goal through the use of relatively more sophisticated acoustic techniques than have generally been applied for this problem in the past. The relationship between cavitation noise and erosion has been studied in recent years in several laboratories (3-9), eg.) for the purpose of eventual prediction of cavitation damage rates from such acoustic measurements. To date no very general success has been attained in this regard. Rather a relatively good relationship between noise level and damage rate for specific units has been observed, so that they could be "calibrated" in this regard. It is our purpose to improve the

the general applicability of acoustic measurements for damage rate prediction by a more pertinent and sophisticated analysis of the acoustic data. Rather than using total noise amplitude, or amplitude within a fixed frequency band, for this prediction, as has been the general practice in the past (3-6, eg.), we propose to analyze the "noise" in terms of a "spectrum" comprising the number of pressure pulses and their individual amplitude. We feel that this additional sophistication will lead to much more generally applicable results, since it is obvious that a total noise amplitude, even within a fixed frequency band, can result from either a very large number of low amplitude pulses or a much smaller number of highly intense pulses. However, presumably only pulses with intensity above a given threshold will contribute significantly to cavitation damage. This general idea is illustrated schematically by Fig. 1 published by the present author in 1963 (9) for cavitation in a venturi, but repeated here for convenience. The anticipated pulse-count spectra are shown schematically in Fig. 2, where number of pulses are plotted against pulse amplitude.

It is anticipated that the pulse-count spectrum "areas", i.e., area under a pulse number vs. energy per pulse curve such as Fig. 2, which represent the total measured energy of the cavitation field, can be correlated with measured erosion energy in terms of measured volume loss per unit exposed area. In the erosion literature this is normally considered in terms of "mean depth of penetration rate", MDPR. The ratio of cavitation field energy (or power) to erosion energy ( or power) then defines a "cavitation

erosion efficiency", which is in principle measurable in laboratory test devices, assuming that the necessary acoustic and electronic instrumentation is provided. Similar instrumentation, installed in prototype or field machines, would then allow an à priori prediction of eventual damage rates to be encountered in such machines. Of course, it would also be necessary to assume that the "cavitation erosion efficiency" remained constant, at least to a degree of engineering utility, between model or other laboratory test, and prototype or field machine. There seems no reason to suppose that this assumption is not sufficiently valid for present purposes. At least it can be checked and evaluated in the research here described. Further, cavitation damage "scale effects" of velocity, pressure, temperature, size, etc. can be predicted from the comparison of the pulse count energy spectra.

The use of bubble collapse pulse spectra for damage prediction is not entirely new in that some related preliminary results are reported from Japan (7,8, eg) and Russia (9).

## II. Experimental Apparatus

### A. Acoustic Instrumentation

Figure 3 shows the type of direct-submergence pressure microprobe used for the detecting and measuring of bubble collapse pressure pulses. This particular unit (of our own design) is fitted with a PZT crystal at the submerged end, sealed from the cavitating liquid by a thin stainless steel diaphrapn. It is suitable for liquid temperatures in excess of 1000°F, and hence could be used for moderately high-temperature sodium, as well as

in water at any temperature of interest. It is suitable for signal frequency of ~10 mH and hence is adequate for measuring cavitation bubble pulses, since the duration of the critical part of the collapse is ~ 1-2 μs. However, very recent research (10) indicates the width of bubble-generated shock waves in water may be as small as ~ 20 nanoseconds. A commercial Kistler micro-probe was also used for some of the water tests. A "wave-guide" probe, i.e., stainless steel rod with crystal fixed at non-submerged end, was used for the sodium tests here reported due to unavailability of the PZT probe (Fig. 3) at that time.

The electronic circuitry used with the wave-guide probe in a vibratory cavitation damage facility in sodium is shown in Fig. 4. This includes a high-pass filter, useful to ~80 kHz, which was particularly necessary for the vibratory facility tests to suppress the 20 kHz imposed driving frequency. It is still possible to measure bubble collapse pulses, since their width is ~ 1-4 μs. The filter will also be used in the venturi tests to suppress all miscellaneous low frequency signals which originate from conventional flow and machinery noise, but presumably do not contribute to cavitation damage. A "pulse-shaper" is also desirable to suppress spurious signals, and allow the electronic counting of only the bubble collapse pulses. This component was not used in the sodium tests because of the uncertain and complex behavior of the wave-guide probes there used as compared to direct-submergence probes as shown in Fig. 3.

B. Vibratory Damage Facility

The most convenient and most common device for testing cavitation damage resistance of various materials is certainly the "vibratory" (sometimes called "ultrasonic") facility. This device and test have in fact recently been standardized by ASTM (11) for water at ambient conditions and the standard is now being extended to other liquids, and pressures and temperatures other than ambient. However, since it is essentially a no-flow device, it is not easily possible at present to utilize these results for the prediction of damage in flowing systems. One of the major purposes of the present research at the U-M is to develop a method for making this prediction, based upon the pulse-count energy spectra here described.

For our own purposes, a relatively standard vibratory horn facility (20 kHz, but here used at double-amplitude, A = $\sim$ 38 $\mu$m rather than the standardized A $\cong$ 51 $\mu$m) has been used for damage tests both in water and in sodium. A static suppression pressure ($P - P_v$) range of 1.5, and the maximum possible temperature range, were used. Earlier results for water over a larger suppression range and at standard double amplitude ($\sim$51 $\mu$m) were reported previously (12,13), and will not be repeated here. Present results for water at 38 $\mu$m amplitude were generally similar, and Fig. 5 shows the effect of amplitude, indicating that damage rate varies approximately as $A^{1.2}$. For the present tests, the wave-guide probe was installed with its tip at the same elevation as the damage specimen face, and at a lateral distance of 3.8 cm. Figure 4 shows schematically this arrangement.

C. Cavitating Venturi Facility

The cavitating venturi facility used for the present research is a portion of our High-Speed Cavitation Tunnel (14). The basic venturi flow-path is shown in Fig. 6. A cylindrical throat (2 cm. nominal diameter, and of 2.25 L/D) is separated by conical sections of 6 deg. including angle. Cavitation originates at throat discharge, and its extent into the diffuser section depends upon pressure and velocity settings. Throat velocities up to ~ 65 m/s can be obtained in tis facility; hence it is very suitable for cavitation damage tests. Water temperature variation from ~15 - ~ 160°C is possible. Deaereation is provided, and total gas content is measured by a Van-Slyke apparatus. Sonic micro-transducer (Fig. 3, eg.) are installed in the cavitating region of the venturi, as are thin-plate damage specimens (Fig. 6). In additions, damage probes installed flush with the venturi wall in position symmetrical to the acoustic micro-probes will also be used.

## III. Cavitation-Erosion Efficiency and Pulse Count Spectra

### A. General

As stated in the Introduction, it is proposed to develop a "cavitation erosion efficiency, $\eta_{cav}$, which relates the acoustic power as measured by a micro-pressure probe installed in the cavitating region (as, eg., Fig. 4 for our vibratory facility) to the "erosion power" measured by the product of erosion volume loss and failure energy per volume of the eroded material, as, eg. (Volume loss) x (ultimate resilience), where ultimate resilience* (UR) is presumed to be the best present measure of material failure

*$UR \cong (TS)^2/2E$, where E is elastic modulus and TS ultimate tensile strength of the material.

energy for cases of cavitation or liquid impingement erosion (15-18, eg.). If later research indicates other mechanical material parameters having the same units, i.e., energy/volume = "stress", to be more suitable in specific cases, then these could be easily substituted into the frame-work of the presently proposed model. For example, it has recently been suggested that the product of ultimate resilience and Brinell hardness (BHN) provides a closer correlation with damage rate (19) than UR alone. In that case, BHN could be converted into an equivalent tensile strength, TS, and the term $(UR \cdot TS)^{1/2}$ could then be used in place of UR, as previously suggested. For purposes of the present paper, however, it will be assumed that UR is the most suitable failure energy parameter.

Acoustic energy as measured by the micro-probe is admittedly at best proportional to the total acoustic energy radiated from the cavitating field, since its output depends upon geometrical factors; fluid factors, etc. However, if the probe can be installed flush with the surface to be damaged, these difficulties are obviously considerably alleviated. In our vibratory facility, (Fig. 4 ) this was not possible, but it is possible for the venturi (Fig. 6 ). A comparison between pulse count and erosion data from both of these facilities should allow an estimate of the effect upon cavitation pulse energy of the specific geometrical difference of the two set-ups, so that the vibratory results can thus be related precisely to the flowing system results. The complex problem of probe installation in rotating machines is not unsolvable, but it is beyond the scope of the present paper.

As previously indicated, the total pulse-count energy can be computed by summing the area under a spectrum curve (Fig. 2). This "spectrum area" can be related to energy in absolute units only by probe calibration. Such calibration was accomplished for the "wave-guide" probes used in the present vibratory sodium tests by impacting the probe with a pendulum-hammer device, for which the input energy could be easily computed from the initial elevation of the pendulum. Thus the "spectrum areas" are known in absolute energy units (20, 21, eg.). From these data, the "cavitation energy" was then computed.

The "erosion energy" was computed directly from measured volume loss and the ultimate resilience of the material (type 304 stainless steel in this case), corrected for test temperature (up to 550°C). From these results, "cavitation erosion efficiency" was then computed, as discussed later.

B. Vibratory Facility Erosion Results

Figures 7 and 8 summarize vibratory facility sodium damage results as a function of liquid temperature and suppression pressure. The trends are typical for any liquid yet tested (12, 13, 22, eg.), showing an optimum damage temperature, with strong decreases of damage for either lower or higher temperature, even for constant suppression pressure. However, a detailed discussion of the reasons for these "thermodynamic effects" is beyond the scope of this paper.

Figure 7 summarizes all presently available vibratory facility damage data for sodium (21,23). Most of this information was previously published in the open literature by the first author (23), but some additional information has not yet been so published (21). Results for several materials (stainless steels types 304 and 316, titanium, Stellite-6, and Colmonoy) and from several laboratories including slightly differing facilities, including our own, are presented. The major point of interest from the present viewpoint is that the overall temperature effect trend is the same for all materials and laboratories, but the "maximum damage temperature" varies between 200 and 400°C depending upon the material tested, and details of the vibratory facilities used.

Figure 8 shows the particular results obtained here in the present investigation (21) for 304 stainless steel for suppression pressures of 2 and 3 bar. While the general temperature trend, is the same as shown in Fig. 7, where only 3 bar suppression pressure was used, there is an increase in damage for the maximum test temperature (550°C). Since our own tests on 316 stainless steel were terminated at 500°C, no direct comparison at 550°C is possible. We attribute the damage increase at this maximum temperature to substantial weakening of the test material (304 SS which is inferior to 316 SS used in the previous tests at very high temperatures), and also to possibly substantially increased corrosion effects at such high temperatures. We believe that this result does not indicate an increase of the mechanical component of the cavitation attack at maximum temperature since the "pulse count spectrum area" (Fig. 9) did not increase, and

since such a conclusion would be counter to all previous theoretical and experimental information concerning the "thermodynamic effect".

A direct comparison between water and sodium in the U-M vibratory facility (23) shows that at the respective maximum damage temperatures, sodium is $\sim$ 2.5 more damaging than water. Of course comparisons at any given temperature are more or less meaningless.

Figure 8 also shows the effect of suppression pressure in the vibratory facility, ie., an increase in suppression pressure in the range tested results in a substantial increase in damage rate. This is confirmed by numerous previous tests with other fluids here and elsewhere (12,13,22,eg.). This is consistent with the overall expectation concerning pressure effect upon cavitation damage in any cavitating device, i.e., there is an optimum damage suppression pressure as well as temperature. This is obvious when it is considered that very high suppression pressure eliminates cavitation entirely, whereas very low suppression pressure eliminates the driving pressure necessary for bubble collapse, i.e., a case of "boiling" rather than cavitation results. These remarks are also consistent with general pump experience, where it is often observed that maximum damage rates result for cavitation conditions near inception. From another viewpoint, it is possible that in some cases an increase of NPSH may result in an increase in damage rather than the anticipated reduction. All such cases must be considered with extreme care if cavitation damage is a consideration.

C. Vibratory Facility Pulse Count Results

Figure 9 shows pulse count spectrum area vs. temperature for the vibratory sodium erosion data resulting in Fig. 8. It is noted that the general shape of pulse count area (Fig. 9) and MDPR (Fig. 8) curves are very similar, indicating a strong positive correlation between these two parameters, as shown over a broader range in Fig. 10 explained later. Spectrum area (Fig. 9) does not show an increase at maximum sodium temperature (550°C) as did WLR (weight loss rate), Fig. 8. This confirms our previous statement that the increase in measured damage at the maximum temperature results from reduction of material mechanical properties and increased corrosion, rather than increased cavitation intensity.

Figure 9 shows data only for 3 bar suppression pressure, but the effect of suppression pressure upon pulse count spectrum area was approximately the same (24) as the pressure effect upon WLR (or MDPR, which are equivalent, since only one material was involved in these tests). References 20,21, and 24 present full details of these tests, which are too voluminous to include here.

Figure 9 contains the legend "90 kHz", indicating that the high-pass electronic filter setting was 90 kHz, approximately the maximum possible for this piece of equipment (Fig. 4). It was generally found that data scatter was reduced for higher filter settings, presumably because of the more effective suppression of the 20 kHz horn driving frequency. All previous

information indicates that the important components of cavitation "noise" from the damage viewpoint is at least ~1 mHz (7-10, eg.).

Figure 10 shows the overall correlation obtained in our vibratory facility between "pulse-count area" and MDPR for both water and sodium (21, 24). The actual data points are included here for simplicity only for sodium. Each data point represents averaged results from one of the temperature and suppression-pressure (2 or 3 bar) combinations tested. In all cases the horn double amplitude is 38 μm and the material 304 SS. Unfortunately facility limitations prevent any overlapping of sodium and water data. However, at all pressures and temperature tested, both water and sodium are well correlated by the same curve. Some effect of high-pass filter setting was noted (Fig. 11) but Fig. 10 is limited to the 90 kHz filter setting.

Figure 11 shows the final correlation achieved between pulse spectrum area and MDPR. The sodium MDPR data points have been increased by a factor of 1.5, assumed the approximate ratio between average and maximum MDPR for this type of test. Due to the difficulty of obtaining sufficiently numerous weight loss data points for sodium to measure directly $MDPR_{max}$, only $MDPR_{aver.}$ was found. It is then necessary to correct to $MDPR_{max}$ to be consistent with the water data, where many more points were available.

Figure 11 also shows the effect of filter cut-off frequency setting and two points labelled "W-ARD Venturi" (also in Fig. 10) These are derived from venturi cavitation damage tests conducted at Westinghouse (25) with sodium temperatures of 370 and 595°C

at the same velocity and cavitation condition. Pulse count areas were computed for these tests using the same "wave-guide" probes used in our own tests. No direct comparison is possible considering the vast geometrical differences involved. However, if one of these W-ARD points is "forced" to lie upon the U-M curve (Fig. 11), the other point also is very close to the U-M curve, as shown in Fig. 11. Thus the curve-fitting relation derived between spectrum area and MDPR from the U-M vibratory tests (Fig. 10) would have allowed a close prediction of the second W-ARD point from the first. This confirms to some extent the usability of the pulse count damage prediction technique for flowing systems from the present vibratory results.

It is also noted (Fig. 10) that the relation between pulse count spectrum area and MDPR is approximately linear for low intensities, but becomes exponential for higher intensity. The linear relation between "area" and MDPR is as expected, since both are based upon energy concepts, and leads to the concept of "cavitation erosion efficiency" discussed later. The exponential relation for higher intensities may be due to the complicating nature of repeated blows upon the surface leading to primarily fatigue-type surface failures, which are no longer proportional to imposed energy.

D. Cavitation Erosion Efficiency

A "cavitation erosion efficiency", $\eta_{cav}$ has been defined here as the ratio between cavitation erosion power (as computed from the product of measured volume loss rate and ultimate resilience) and fluid acoustic power (as measured by a micro-pressure-probe installed in the approximate region where erosion occurs). The eroded area used for computation of "erosion power" is considered to be equal to that of the micro-probe tip (Fig. 3) through which the pressure pulse signals are received. The method of computing "acoustic power" is outlined in the foregoing and described in full detail in previous project reports (20, 27). As previously discussed here, the acoustic power is proportional to the pulse-count spectrum areas, correlated with measured MDPR in Figs. 10,11. The necessary probe calibration to reduce "area" to energy or power units was accomplished using a hammer-pendulum device (20) to impact the probe tip. This device provides loading rates at least somewhat similar to bubble collapse pressure pulses.

Figures 12 and 13 show computed cavitation erosion efficiency, $\eta_{cav}$ as a function of sodium liquid temperature from our vibratory facility for 2 and 3 bar suppression pressures, and for 70 and 80 kHz filter cut-off frequency settings. At this point it is not known whether or not the trends shown are significant, since many further tests and comprehensive analysis yet to be done will be necessary to determine that point. The major point of significance now is indicated magnitude of $\eta_{cav}$, which is $10^{-8}$, but which remains within a factor of $\sim 5$ for all conditions tested.

No comparisons with other results are possible, since no previous work of this sort is known to the authors. Intuitively it would be expected that the "erosion efficiency" would be small. Simple calculations indicated that this must be the case, since otherwise very much larger cavitation erosion rates would be observed than is actually the case. The approximate order of the acoustic power for these tests ($\sim$10 watts) seems reasonable since vibratory horn input power is of the order of 200 watts, and that computed for the fluid near the horn tip of the order 100 watts.

An extremely low "erosion efficiency" is also consistent with results of high-speed motion picture studies of cavitation fields, conducted here (28,29 eg.) and elsewhere, which indicate a ratio of the order $10^4$-$10^9$ between the number of bubbles observed collapsing near a specimen surface and the number of individual pits and craters found in specimen materials. This work (28) showed a calculated ratio of bubble energy to pit erosion energy ranging from $10^9$ to $10^{13}$ for tests in a venturi with water and mercury. Thus the presently computed erosion efficiency of $\sim 10^{-8}$ seems roughly consistent and plausible from whatever scanty past information is available.

## E. Venturi Tests and Bubble Collapse Pulse Characteristics

### 1. General

As previously mentioned, cavitating venturi tests have been conducted in this laboratory (14,28,29, eg.) for many years. For the most part these have used the same general venturi geometry (Fig. 7) with or without damage test specimens.

In-depth damage studies on numerous materials were conducted (28,29, eg.). Similar tests are being continued under the present research program, but no new damage data is available, for conclusion in this paper. The new damage tests, however, will be correlated with venturi pulse count spectra as described in the previous sections. Thus the correlations already presented including "cavitation erosion efficiency" (Figs. 9-13) can be verified or modified in light of this new data from a flowing system. Eventual further verification and comparison from tests in other laboratory flowing and field systems are planned. The present work has already produced significant information on pulse and pulse spectra characteristics, as discussed in the following.

2. Venturi Pulse Spectra and Pulse Characteristics

Figure 14 shows a typical bubble collapse pulse count spectrum (30), showing number of bubble collapse pulses vs. pulse amplitude, obtained using a Kistler micro-probe inserted in our cavitating venturi. A conventional nuclear scalar and multi-channel analyzer with suitable "pulse-shaper" were used to obtain this data. While the absolute magnitudes are not available, the general shape of the curve is as expected, i.e., a maximum number of pulses of reduced amplitude with a reducing number of pulses at higher amplitudes, following a relatively smooth curve out to relatively high amplitudes. Presumably it is this high-amplitude portion of the curve which is primarily responsible for cavitation damage.

Figure 15 shows typical pulse outputs from the U-M probe (Fig. 3), indicating that, as measured by this probe, the pulses have a typical width of $\sim$1-4 $\mu$s. Calculations (31, eg.)

and measurements with more sophisticated probes (10, eg.) indicate that their actual duration may often be somewhat less. For present purposes, however, this probe, or a conventional Kistler probe which produces relatively similar results, appears adequate.

Figure 16 shows the effect of a "pulse-shaper" which primarily suppresses the following negative and positive probe outputs resulting from a single bubble collapse. The use of this component will allow a more meaningful pulse count spectrum than would otherwise be possible.

F. Scale Effects From Present Research

1. Vibratory Facility Results

While no new tests on "rotodynamic machines" are here reported, our present studies do allow some useful predictions of trends concerning cavitation damage scale effects. While the "vibratory facility" results here discussed for water and sodium do not allow quantitative predictions for flowing systems, nevertheless the trends shown should be valid. Those which can reasonably be translated into flowing machine predictions are the following.

1) Temperature ("thermodynamic") Effect. It is well accepted (12,13,15,eg), and further verified by these tests, that an "optimum damage temperature" exists for any liquid. While its value depends to some extent upon other test parameters including material properties, it can be postulated as a result of the present tests that it lies between $\sim$200 and $\sim$400°C for sodium and $\sim$40 and $\sim$70°C for water at suppression pressures

of interest. Thus it is within the operating range of pumps for LMFBR, but not so for water-cooled reactors. While the damage decrease at low temperatures is of the order of 50%, it is very much greater for excessively high temperatures, being at least of the range $10^2$ to $10^3$.

2) Pressure (and Velocity) Effects. These tests and others before (12,13,15,eg.) show that there is an "optimum" damage suppression pressure (or NPSH) as well as temperature. Within the range of operation of vibratory facilities, the effect of an increase in suppression pressure is a strong increase in damage rate, roughly proportional to $(NPSH)^2$. However, it is obvious that if NPSH could be increased sufficiently, cavitation damage would fall to zero as cavitation would then be completely suppressed. This is obviously also true for any flowing system, and of course it is the present general expectation that cavitation difficulties are alleviated by increased NPSH. An obvious exception, however, are "super-cavitating" devices, where very low cavitation sigma results in reduced or non-existent damage. It is also a fairly general observation in the pump industry that maximum damage often occurs for a cavitation condition near inception. In such a case, a decrease in NPSH would obviously reduce damage. It is also obvious from careful consideration of these points that an increase in NPSH (or sigma) could substantially worsen the cavitation damage situation. Obviously much further research needs to be done before reasonably confident predictions can be made in this regard.

It is hoped that the concept of pulse count spectra and cavitation erosion efficiency here advanced can substantially alleviate this situation.

The "velocity effect" is obviously intimately connected with the pressure effects discussed above, since pressure changes are normally related to changes in $V^2$. In the case of cavitation, however, the precise relationship between these parameters depends upon many other parameters such as geometry, eg. In a cavitating venturi, eg., an increase in velocity may only extend the cavitating region without any corresponding change in pressure in the region of bubble collapse. In such a case, the "velocity effect" may be greatly suppressed (28,29,32, eg.), and may even become negative. Nevertheless for many roto-dynamic devices, very large "velocity exponents" ($\sim 6$- $\sim 10$) have been observed (33, eg.).

3) Comparison of Water and Sodium Damage Rates. The present vibratory tests allow a direct comparison between sodium and water damage rates in the same facility. No such direct quantitative comparison for flowing systems exists to our knowledge, yet the vibratory results should be qualitatively valid. As already mentioned, damage rate for any liquid is highly temperature dependent for fixed suppression pressure (or NPSH), so that a damage-rate comparison between any two liquids is meaningless unless the relation between test temperature and maximum damage temperature for those particular conditions is known or specified. The most meaningful comparison between liquids such as sodium and water is then in relation to their

maximum damage temperatures. Under these conditions from our vibratory test results, the damage rate for maximum damage temperature for sodium is ~2.5 x that for water, i.e., from an "engineering viewpoint" their damage rates appear to be of the same general magnitude, for the same NPSH. Since densities of water and sodium do not differ greatly, the above stated result would also apply roughly for a comparison at fixed suppression pressure. While no reference velocity is involved in the vibratory test, kinematic conditions are fixed for given horn amplitude and frequency. These were maintained constant for the sodium-water comparison.

4) Prediction of Damage Scale Effects from Bubble Collapse Pulse Spectra. Application of the correlations discussed in this paper between bubble collapse pulse spectra and measured MDPR in laboratory devices through the use of "cavitation erosion efficiency" will allow the prediction of velocity, pressure, temperature, and size damage scale effects in prototype devices, if the same acoustic outputs are measured and reduced in the fashion described in the foregoing. In addition, laboratory flowing tests, such as venturi, rotating disc, etc. can be used to measure the effect upon bubble collapse spectra of variation of these parameters, and hence will allow the "measurement" of their effect upon the mechanical component of cavitation attack. Of course this acoustic output will not reflect corrosive effects. Thus this technique can be used to separate mechanical and corrosive effects in various applications. These can also be measured in laboratory tests, comparing liquids such as tap water, sea water, various

chemicals of interest, etc. Since the mechanical intensity can be measured (acoustically), the effects upon total damage of corrosion or other chemical attack can be inferred by difference.

## IV. CONCLUSIONS

The concept of a "cavitation erosion efficiency", $\eta_{cav}$ is introduced. This is defined here as the ratio between "erosion power" as manifested by the product of measured erosion volume loss rate times a material parameter representing volumetric failure energy , and the cavitation field "acoustic power" as measured by a calibrated micro-probe installed in the cavitating region. "Acoustic power" as here defined consists of the area under a bubble collapse spectrum curve. Ideally, $\eta_{cav}$ is a function only of geometrical parameters concerning the probe location compared to that of the damaged region. Knowledge of $\eta_{cav}$ and the measurement of acoustic power as here described would allow engineering estimation of eventual damage rate in a prototype application for any material, using eventual more extended laboratory results of the type presented in this paper.

Relatively good correlation between "bubble collapse pulse spectra", i.e., "acoustic power" and measured erosion rate for a vibratory cavitation facility is shown from tests in liquid sodium and water over a broad range of temperature and suppression pressure (NPSH/$\rho$). Erosion efficiency, $\eta_{cav}$ is calculated from this data using ultimate resilience, UR as the pertinent material failure energy parameter (based on various previous

tests here and elsewhere), giving relatively constant $\eta_{cav}$ over the range of the tests. The validity of UR for this purpose is not further verified by the present tests, since only type 304 stainless steel was tested.

A direct comparison of sodium and water in our vibratory facility shows that sodium is ~2.5 x more damaging than water, comparing results at the maximum damage temperature for each liquid, and at the same NPSH.

The possibility of an increase in damage for an increase in NPSH, which occurs commonly in vibratory tests, also exists for flowing devices, i.e., there exists an NPSH corresponding to maximum damage rate for most devices. Thus the concept of "optimum" damage pressure as well as temperature applies.

Measured bubble collapse pressure pulses from a cavitating venturi in water show the width of such pulses to be 1-4 μs using our direct submergence micro-probe. A typical pulse spectrum (number vs. amplitude) shows that pulse number decreases strongly for increased strength. Presumably it is the relatively small number of highly energetic pulses which are predominently responsible for damage.

ACKNOWLEDGMENTS

Financial support for these investigations for the most part was derived from Office of Naval Research Contract No. N00014-76-C-0697.

## REFERENCES


1. R. H. Fakkel, etal., "Comparison of Cavitation Test on the SNR 300 Prototype Sodium Pump, Carried Out Using Water at Room Temperature and Liquid Sodium at 580°C", Edinburgh Conf., Proc. Conf. on Cavitation Fluid Mach. Group, I, Mech. E., Scotland, Sept. 1974, p. 341-354.

2. R. H. Fakkel, M. W. Heslenfeld, and J. P. Vroom, "6000 Hours Testing of a Full-Scale Prototype Sodium Pump", Nuclear Engr. Int., Sept. 1973, p. 949-951.

3. I. S. Pearsall, P. J. McNulty, "Comparisons of Cavitation Noise with Erosion", 1968 ASME Cavitation Forum, p. 6-7, ASME, N. Y., N. Y.

4. W. M. Deeprose, N. W. King, P. J. McNulty, and I. S. Pearsall, "Cavitation Noise, Flow Noise and Erosion", Proc. Conf. on Cavitation, Inst. Mech. Engrs., Fluid Machinery Group, Herriot-Watt Univ., Edinburgh, 373-381, Sept. 1974.

5. J. J. Varga, Gy. Sebestyen, "Determination of Hydrodynamic Cavitation Intensity by Noise Measurement", Proc. 2nd International JSME Symp. on Fluid Machinery and Fluidics, Tokyo, Sept. 1972, 285-292.

6. J. J. Varga, Gy. Sebestyen, and A. Fay, "Detection of Cavitation by Acoustic and Vibration-Measurement Methods", La Houille Blanche, 2, 1969, 137-149.

7. F. Numachi, "Transitional Phenomena in Ultrasonic Shock Waves Emitted by Cavitation on Hydrofoils", Trans. ASME, J. Basic Eng., 81, June 1959, p.153.

8. F. Numachi, "An Experimental Study of Accelerated Cavitation Induced by Ultrasonics", Trans. ASME, J. Basic Engr., 87, 1965, 967-976.

9. V. K. Mukarov, A. A. Kortnev, S. G. Suprun, G. I. Okolelov, "Cavitation Erosion Spectra Analysis of Pulse-Heights Produced by Cavitation Bubbles", Proc. 6 th Non-Linear Acoustics Conference, Moscow, July 1975, (Odessa Poly. Inst.).

10. W. Lauterborn and K. -J. Ebeling, "High-Speed Holography of Laser-Induced Cavitation Bubbles in Liquids", Proc. of 7th International Symp. on Nonlinear Acoustics", Aug. 19-21, 1976.

11. "Standard Method of Vibratory Cavitation Erosion Test", Designation G 32-72, ASTM, 1972, (anonymous).

12. F. G. Hammitt, and N. R. Bhatt, "Cavitation Damage at Elevated Temperature and Pressure", ASME Cavitation and Polyphase Flow Forum, 1972, p. 11-13.

13. F. G. Hammitt and D. O. Rogers, "Effects of Pressure and Temperature Variation in Vibratory Cavitation Damage Test", J. Mech Engr. Sci., 12, 6, 1970, 432-439.

14. F. G. Hammitt, "Cavitation Damage and Performance Research Facilities", Symp. on Cavitation Research Facilities and Techniques, p. 175-184, edit. J.W. Holl and G.M. Wood, Philadelphia, Pa., May 18-21, 1964.

15. J. M. Hobbs, "Experience with a 20-Kc. Cavitation Erosion Test", ASTM STP, No. 408, 159-179, 1967.

16. F. J. Heymann, "Toward Quantitative Prediction of Liquid Impact Erosion," ASTM STP No. 474, 1970, 212-248.

17. R. Garcia and F. G. Hammitt, "Cavitation Damage and Correlations with Material and Fluid Properties", Trans. ASME, J. Basic Engr., 89, Dec. 1967, p. 755-763.

18. F. G. Hammitt, and F. J. Heymann, "Liquid-Erosion Failures" , American Society for Metals, Metals Handbook, 10, 1975, p. 160-167.

19. B. C. Syamala Rao, N. S. Lakshmana Rao, and K. Seetharamiah, "Cavitation Erosion Studies with Venture and Rotating Disk in Water", Trans. ASME, J. Basic Engr., 92, D, 3, Sept., 1970, 563-579.

20. M. K. De, S. A. Barber, and F. G. Hammitt, "Pressure Probe Calibration", ORA Rept. No. UMICH 014456-1-I, July, 1976.

21. F. G. Hammitt, etal., "Final Report - Argonne National Laboratory", ORA Rept. No. UMICH 013503-2-F, June, 1976.

22. J. M Hobbs and A. Laird, "Pressure, Temperature and Gas Content Effects in the Vibratory Cavitation Erosion Test", 1969 Cavitation Forum, ASME, p. 3-4.

23. F. G. Hammitt and N. R. Bhatt, "Sodium Cavitation Damage Tests in Vibratory Facility - Temperature and Pressure Effects", ASME Cavitation and Polyphase Flow Forum, 1975, p. 22-25.

24. F. G. Hammitt, etal., "Progress Report No. 3 - Argonne National Laboratory", ORA Report No. UMICH 013503-3-PR, Feb. 1976.

25. P. R. Huebotter, etal., "Principal Results of U. S. Base Technology Program on Cavitation in LMFBR Plants", Trans. ANS Winter Meeting, Nov. 15-19, 1976.

26. T. J. Costello, R. L. Miller, and S. L. Schrock, "Cavitation Test", Progress Report No. W-ARD XARA - 52045, Westinghouse Advanced Reactor Div., June 1976.

27. S. A. Barber, "An Examination of Cavitation Erosion Efficiency", ORA Rept. No. UMICH 014456-5-I, Dec. 1976.

28. M. J. Robinson and F. G. Hammitt, "Detailed Damage Characteristics in a Cavitating Venture", Trans. ASME, J. Basic Engr., 89, D, 1, March 1967, p. 161-173.

29. R. T. Knapp, J. W. Daily and F. G. Hammitt, Cavitation, McGraw-Hill, 1970.

30. O. Ahmed and F. G. Hammitt, "Pressure Pulse Distribution from Cavitation Collapse", ORA Rept. No. UMICH 013503-2-I, March 1975.

31. C. L. Kling and F. G. Hammitt, "A Photographic Study of Spark Induced Cavitation Bubble Collapse", Trans. ASME, J. Basic Engr., 94, D, 4, Dec., 1972, p. 825-833.

32. G. M. Wood, L. K. Knudsen and F. G. Hammitt, "Cavitation Damage Studies with Rotating Disc", Trans. ASME, J. Basic Engr., 89, D, 1, March 1967, p. 98-110.

List of Figures

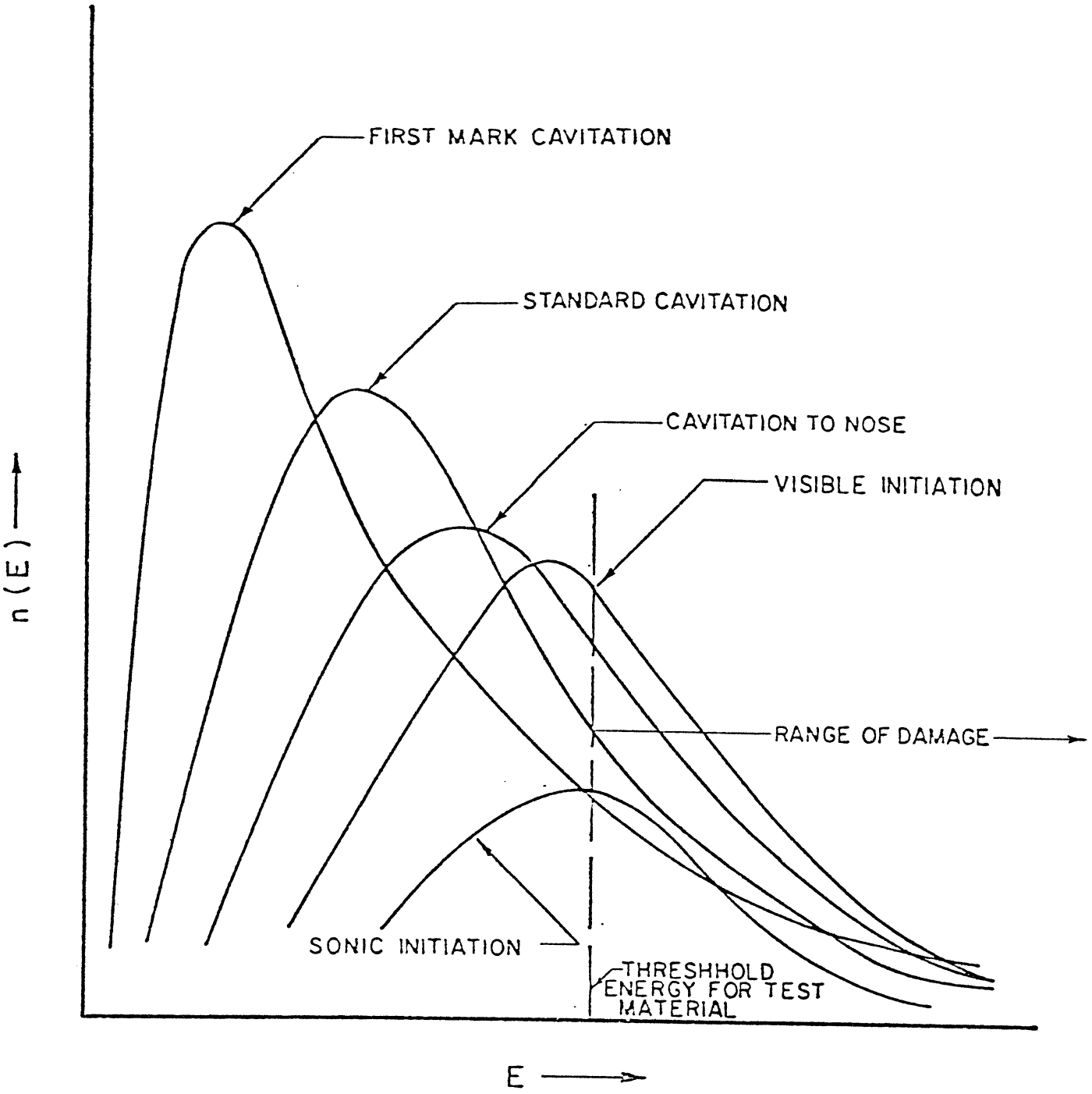


Fig. 1 - Hypothesized bubble energy spectra for various cavitation conditions at a constant velocity, for a given material. Presumably, curves at higher velocity are generally similar, but at higher n(E) and E. The quantity n(E) = number of bubbles from those "in vicinity" of damage specimen which deliver an energy quantum E to the surface of the specimen, and E = energy delivered by an individual bubble to the surface of the specimen.

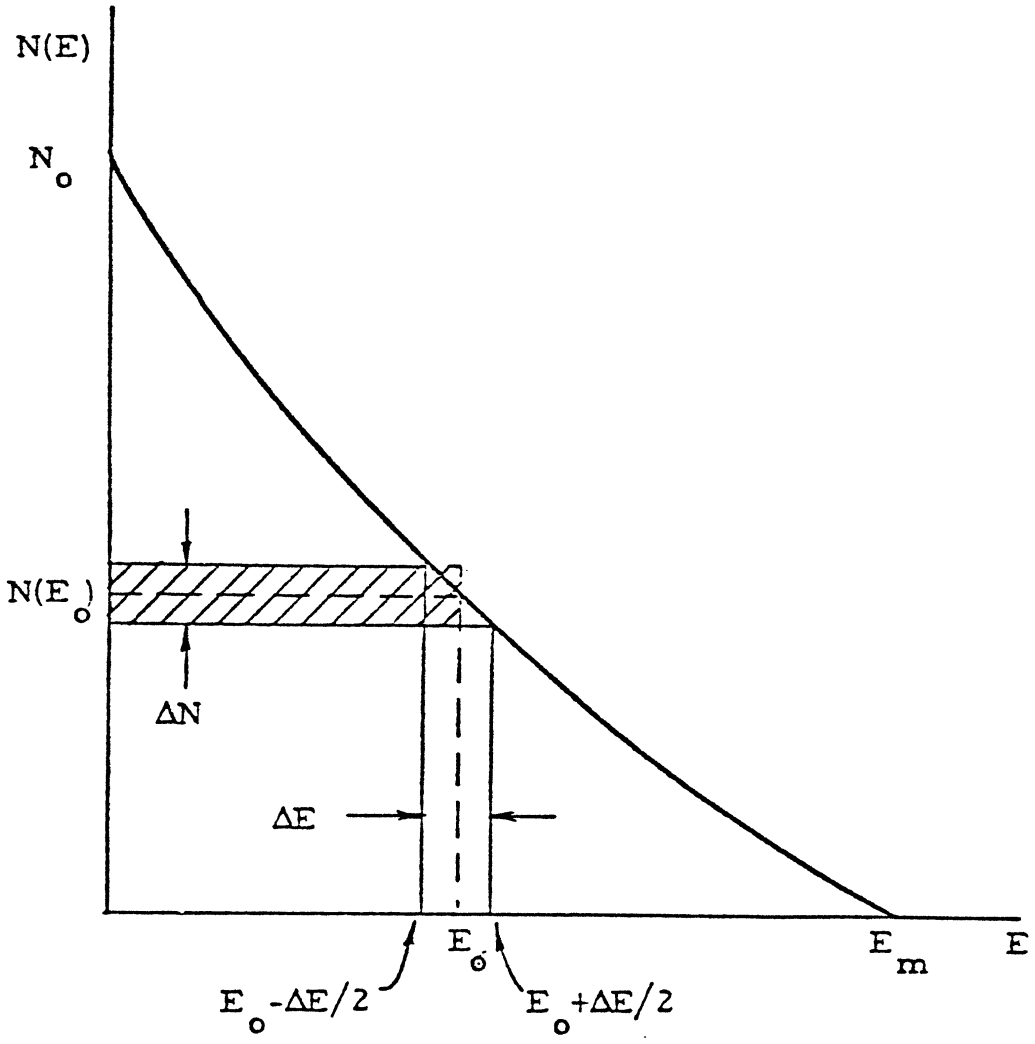


Fig. 2 - Typical Pulse Spectrum.

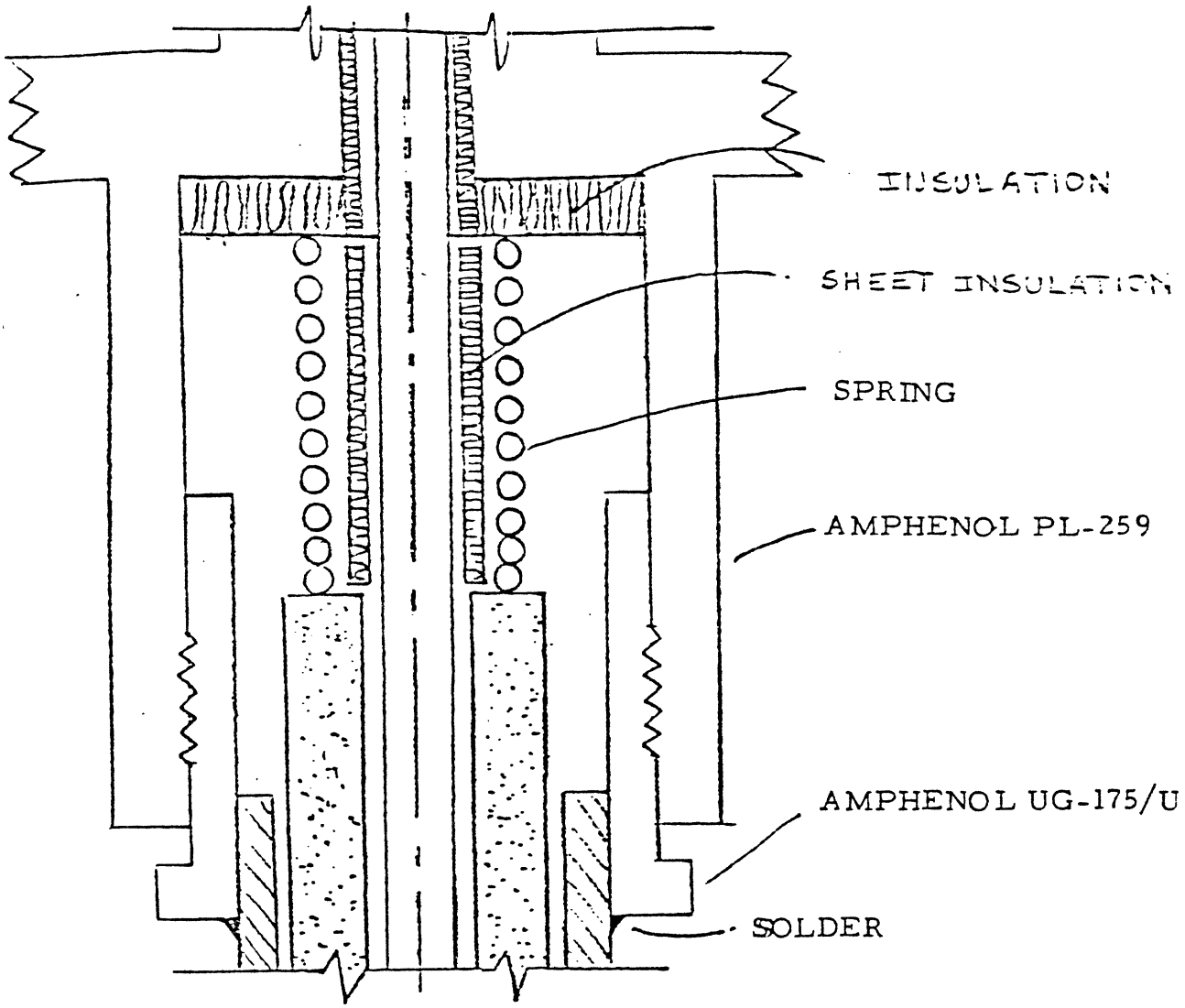


Figure 3

HIGH TEMPERATURE ACOUSTIC PROBE (U-M)

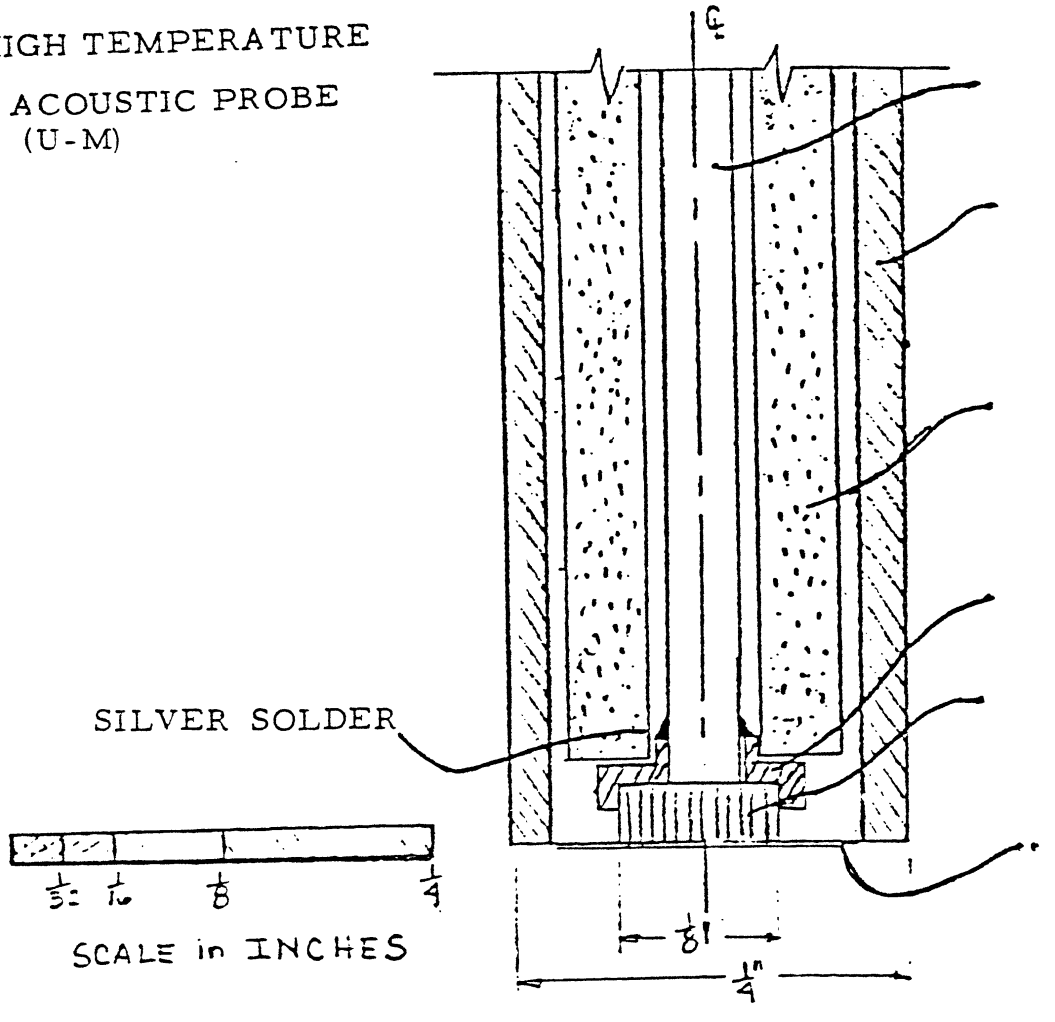

FIG. 4

# BLOCK DIAGRAM OF ULTRASONIC VIBRATORY FACILITY

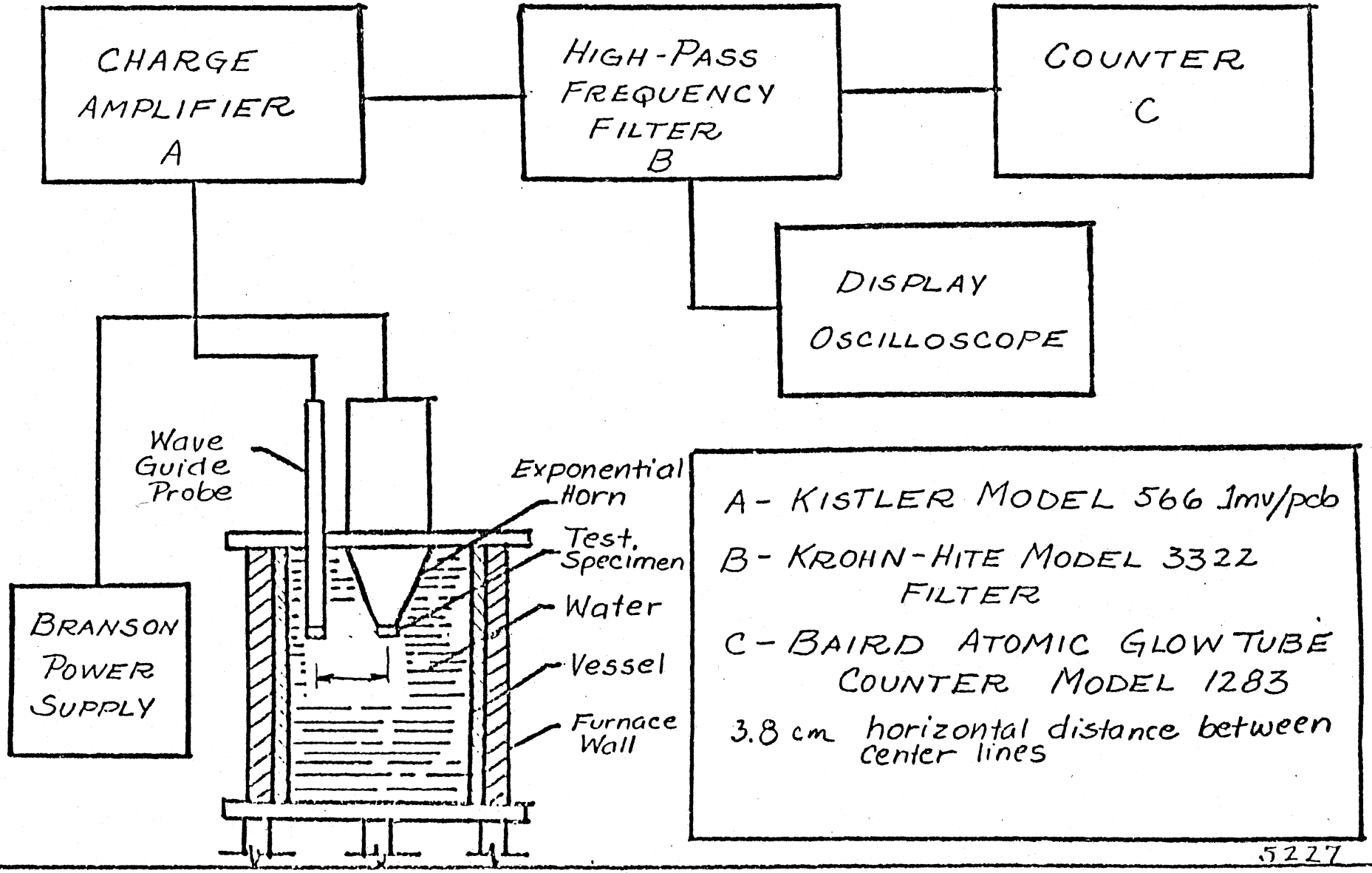


A - KISTLER MODEL 566 1mv/pcb

B - KROHN-HITE MODEL 3322 FILTER

C - BAIRD ATOMIC GLOW TUBE COUNTER MODEL 1283

3.8 cm horizontal distance between center lines

5227

J.A. FAUST 2-19-7

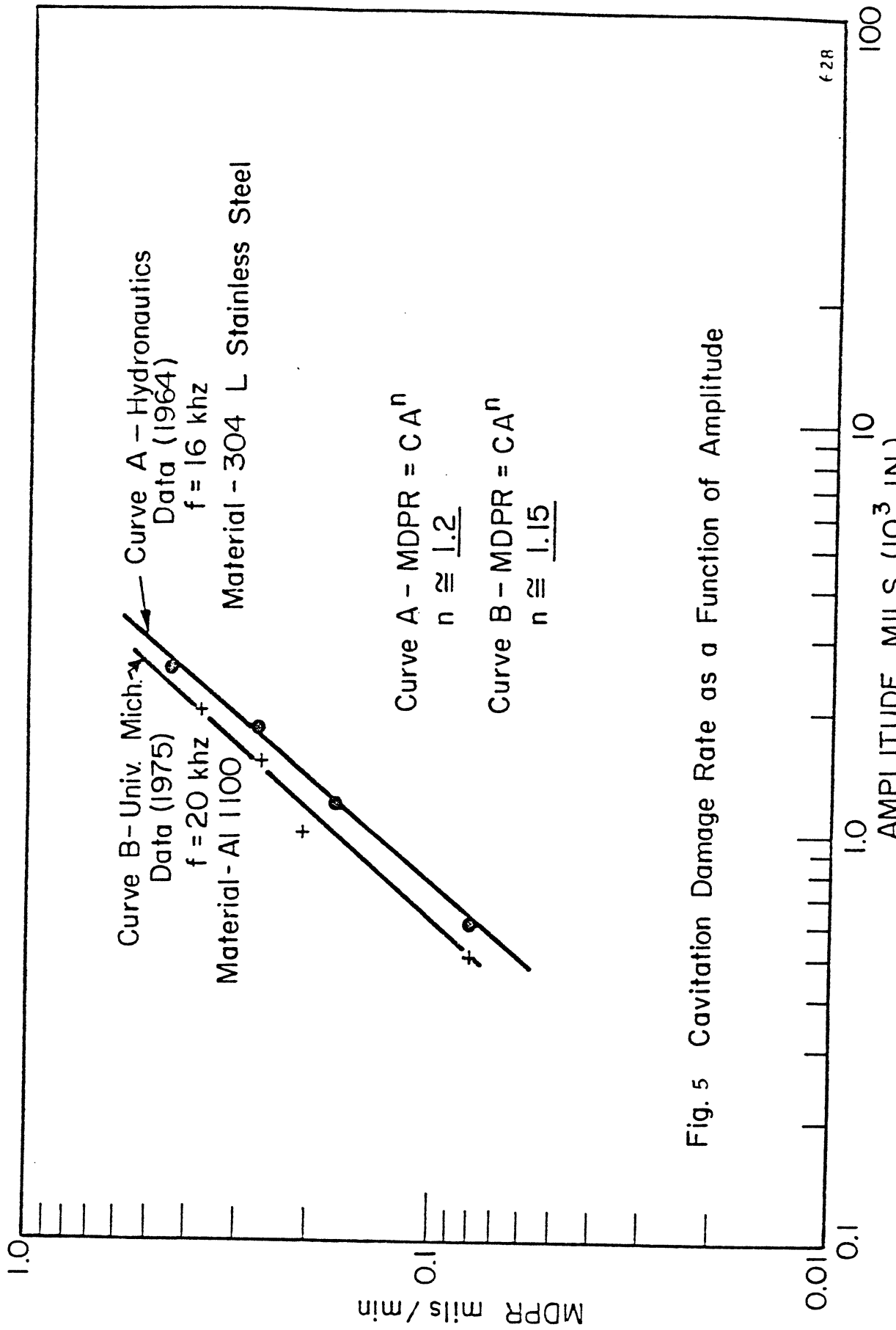


Fig. 5 Cavitation Damage Rate as a Function of Amplitude

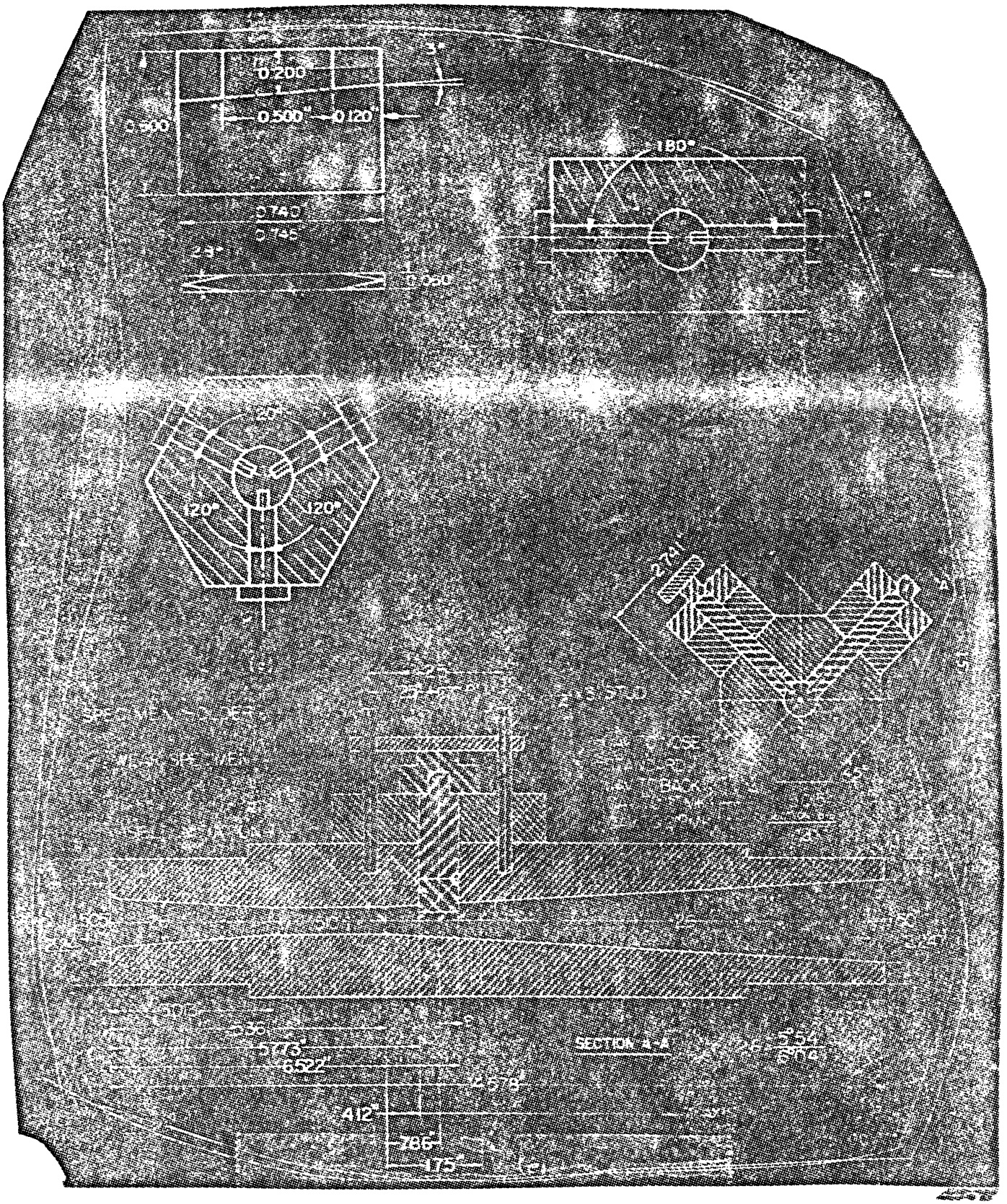


Fig. 6 - Drawing of the Damage Test Venturi showing Nominal Flow Passage and Specimen Location, Cavitation Termination Points, and (a) Test Specimen Dimensions, (b) Two Specimen Symmetrical Arrangement, (c) Three Specimen Symmetrical Arrangement (d) Two Specimen Unsymmetrical Arrangement.

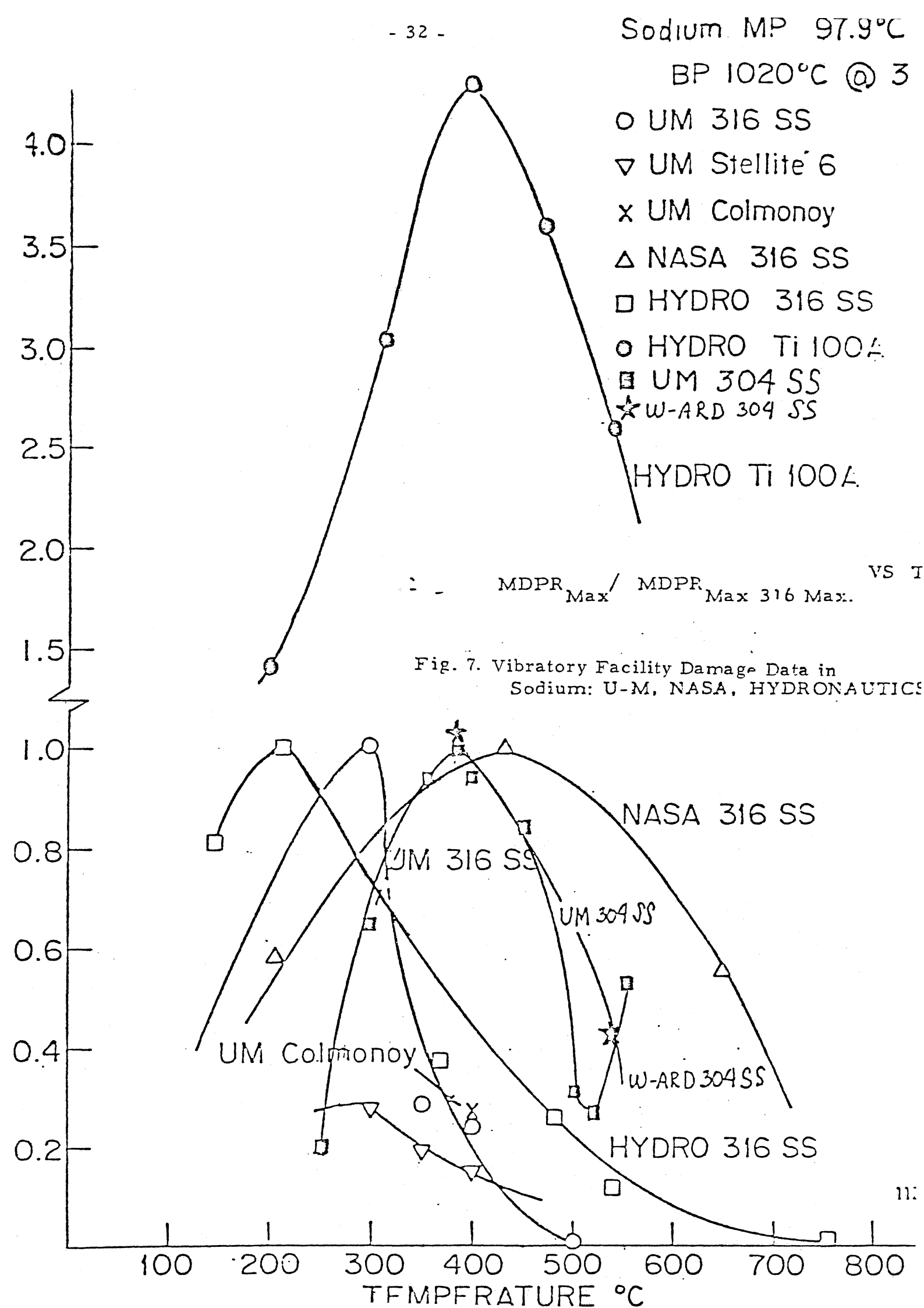


Fig. 7. Vibratory Facility Damage Data in Sodium: U-M, NASA, HYDRONAUTICS

Figure 8

WEIGHT LOSS VS TEMPERATURE

for SODIUM

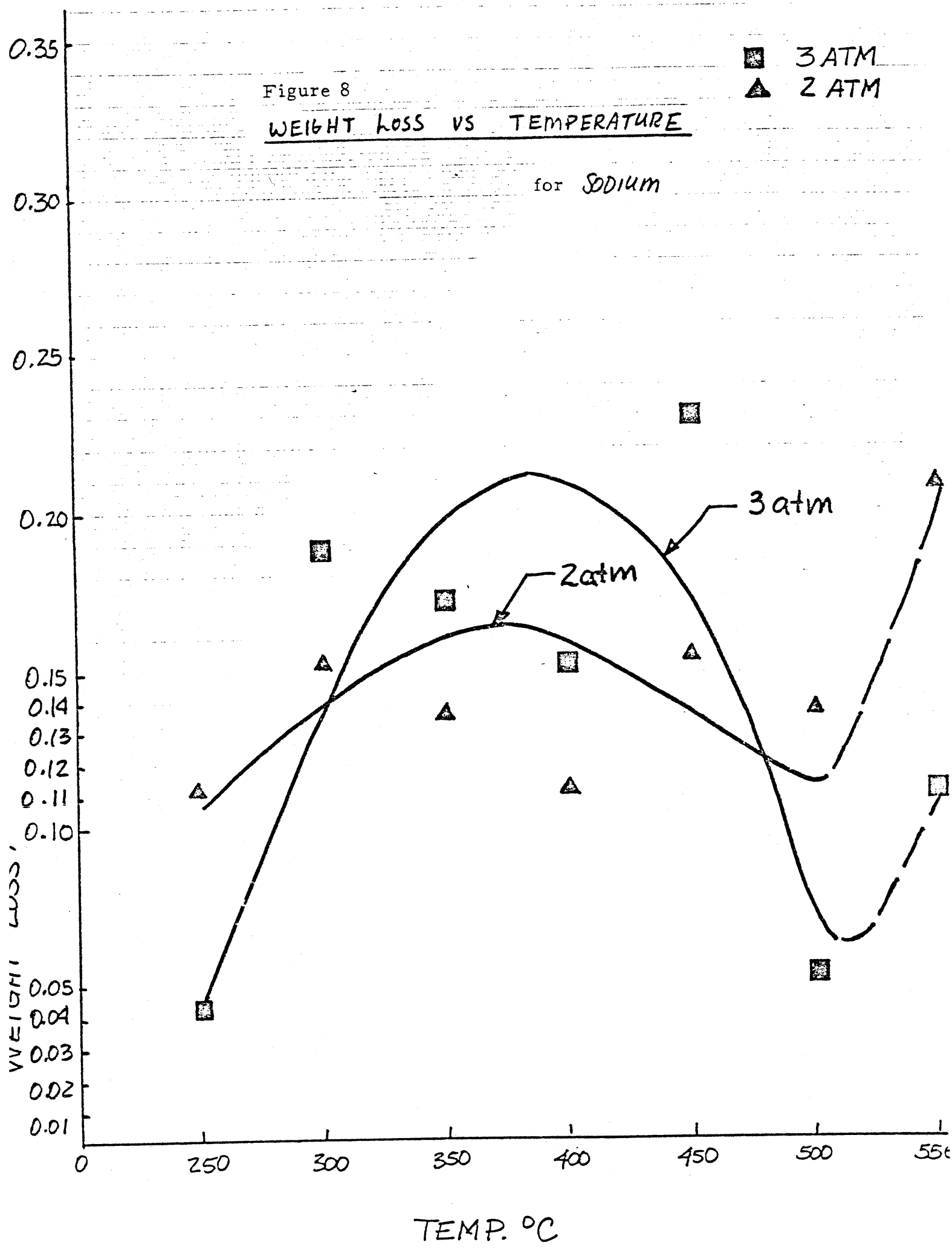

Figure 9 - Spectrum Area vs. Temperature.

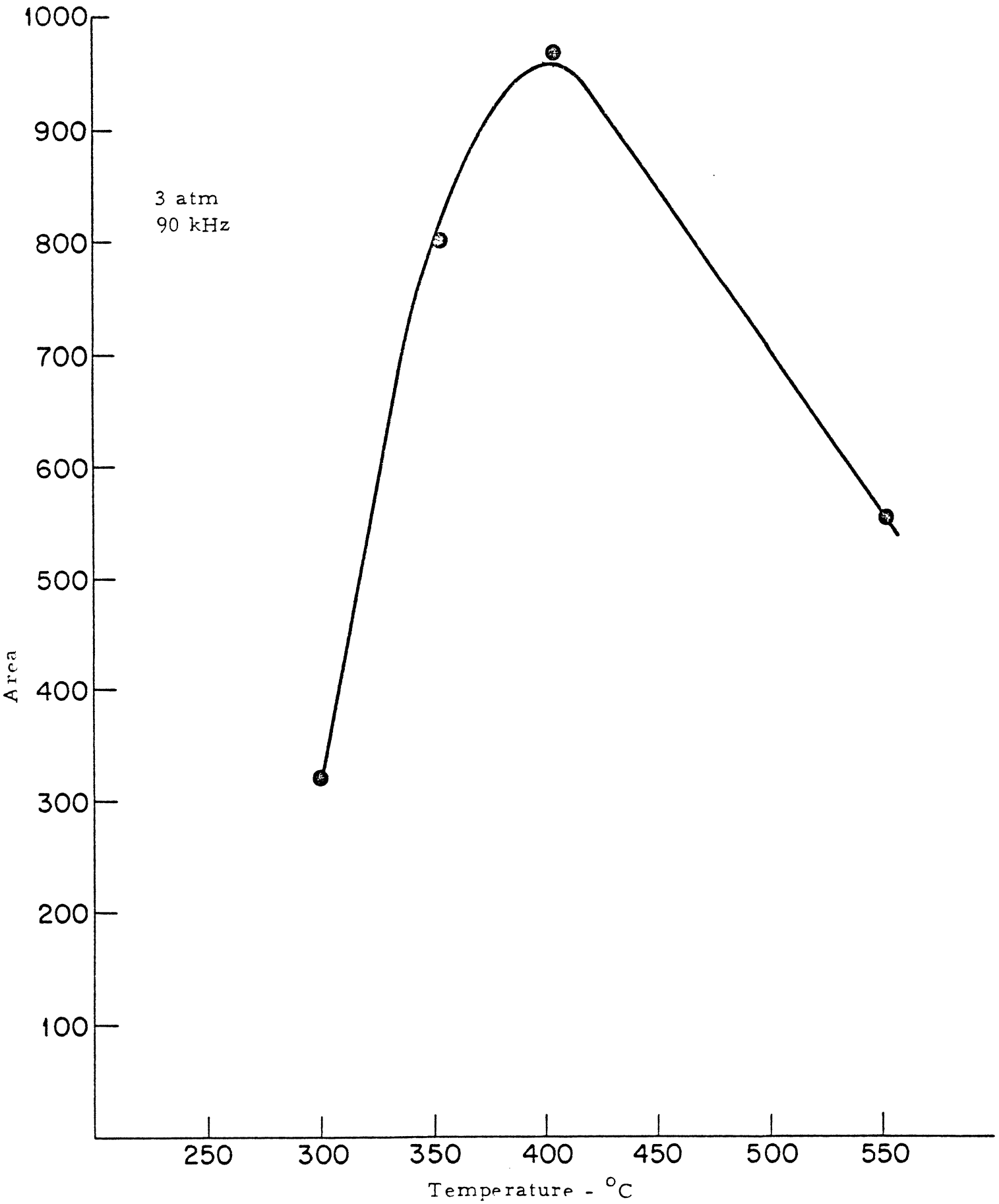

Figure 10 - Correlation of Spectrum Area and MDPR (raw data).

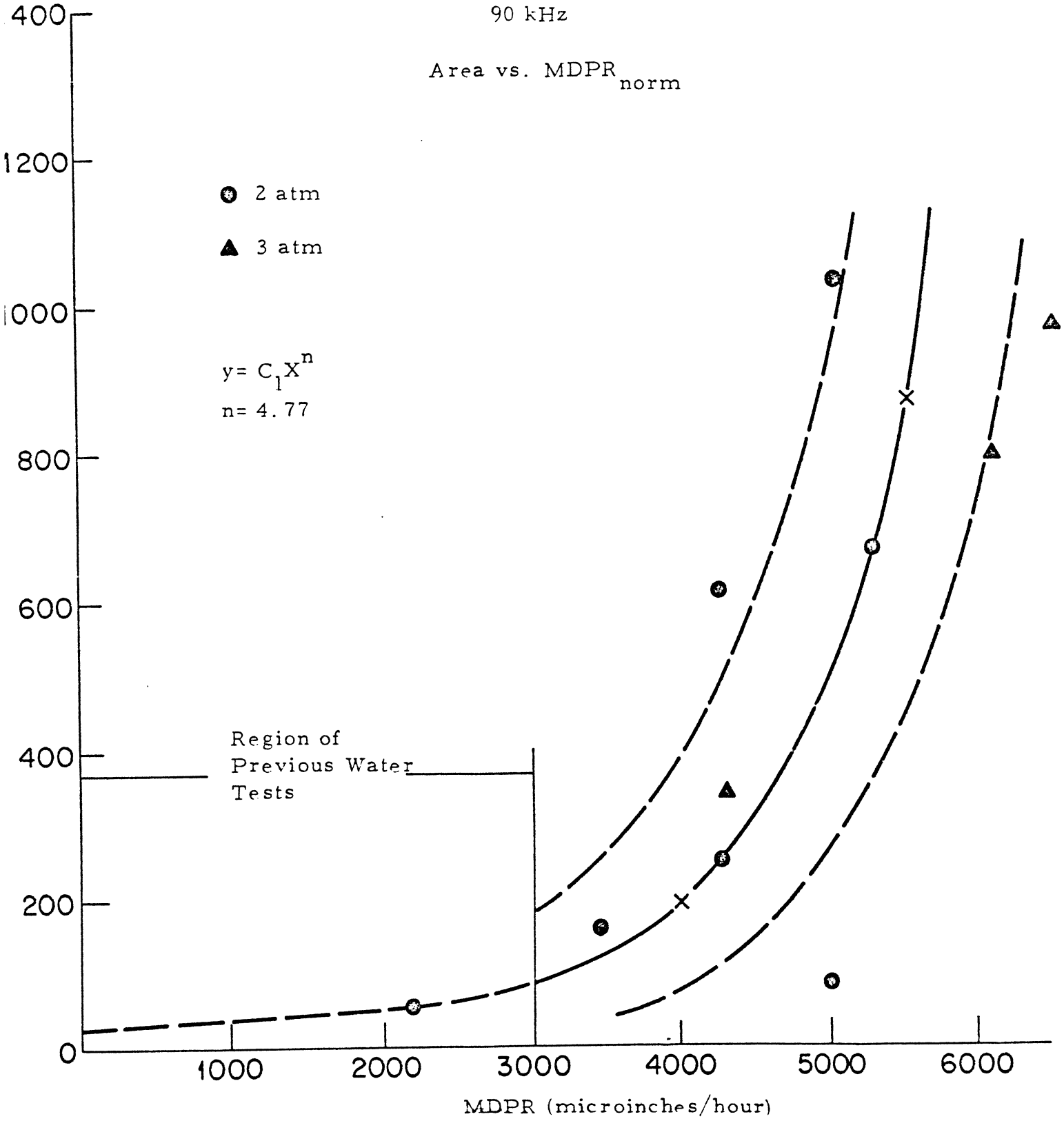

Fig. 11 Final Correlation of Pulse Pressure Spectrum Area and MDPR

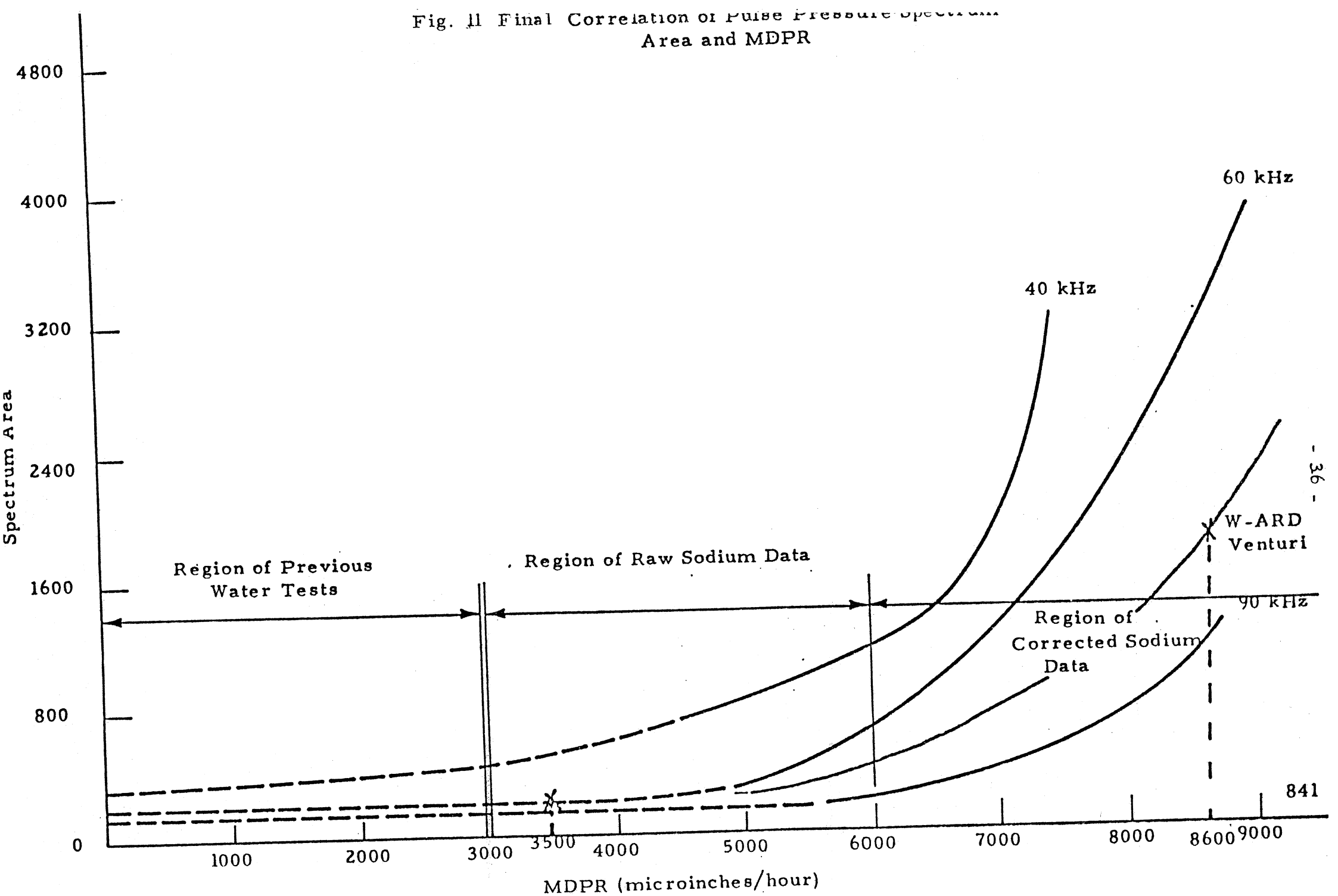

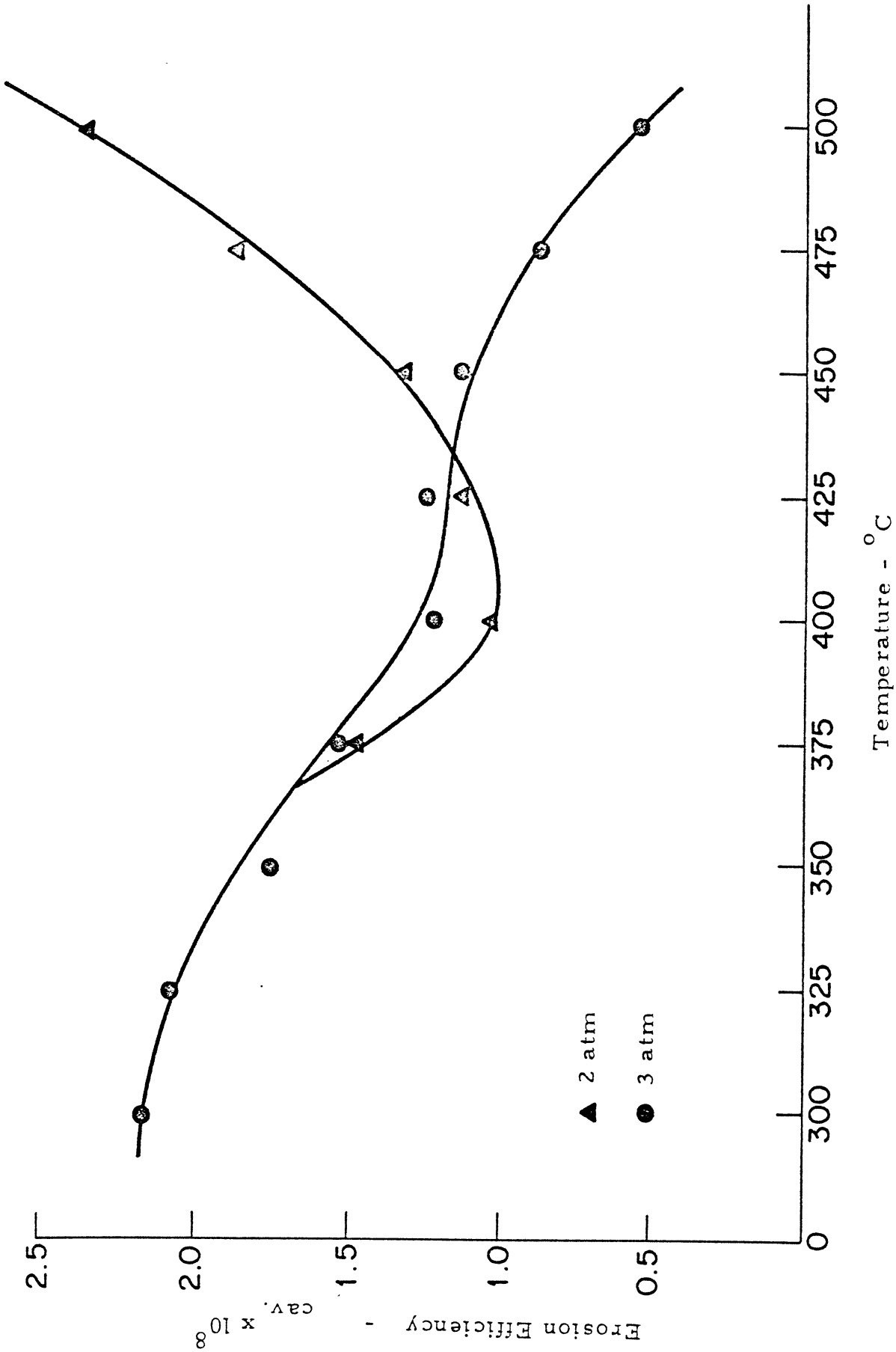


Figure 12 - Temperature vs. Cavitation Erosion Efficiency for 70 kHz.

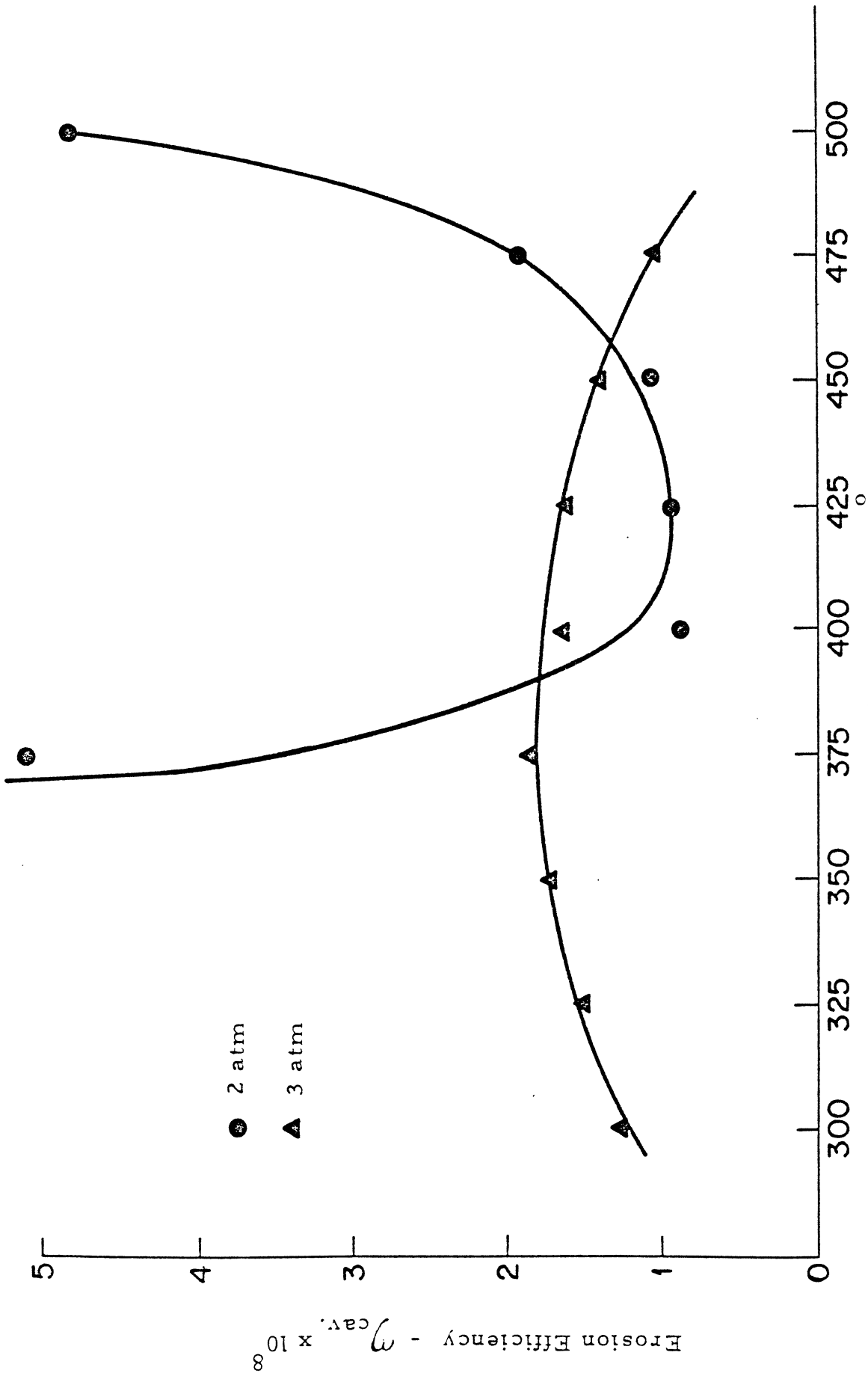


Figure 13 - Temperature vs. Cavitation Erosion Efficiency for 80 kHz.

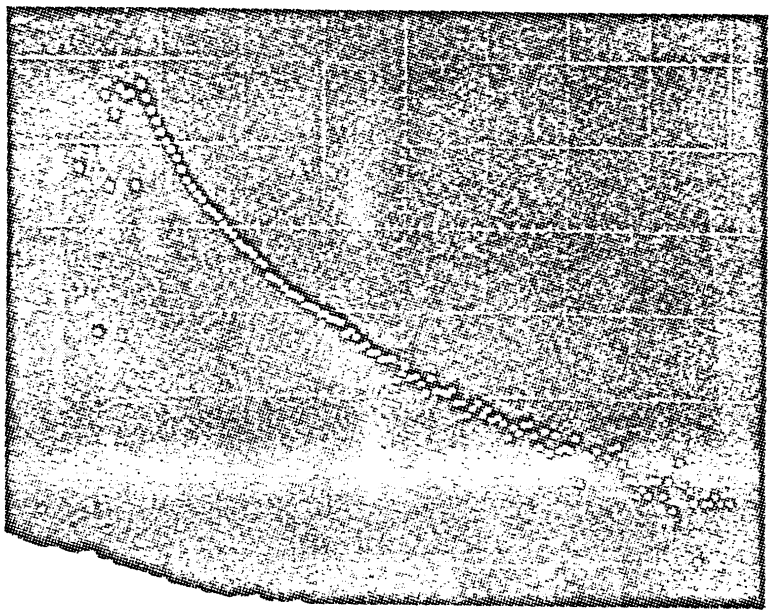

Figure 14 - Spectrum of Pressure Pulses from Venturi (Ref. 30)

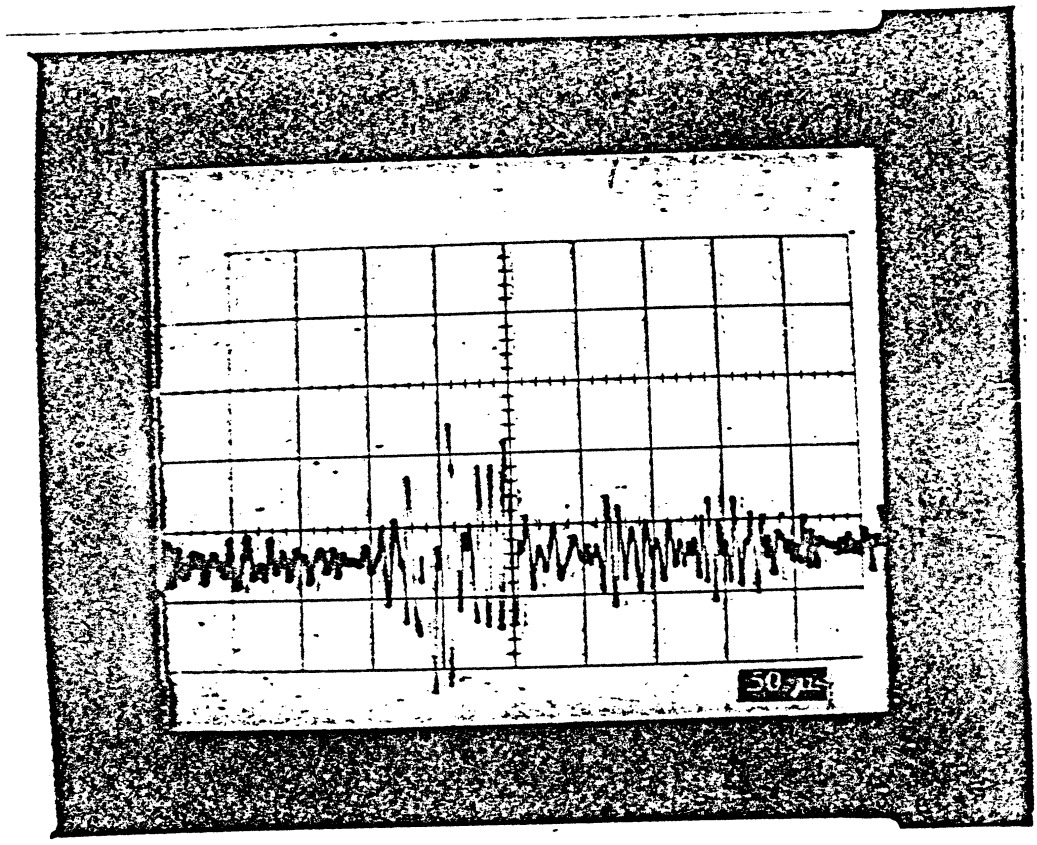


Figure 15 - Oscilloscope Output from U-M Probe in Venturi (no Pulse - Shaper)

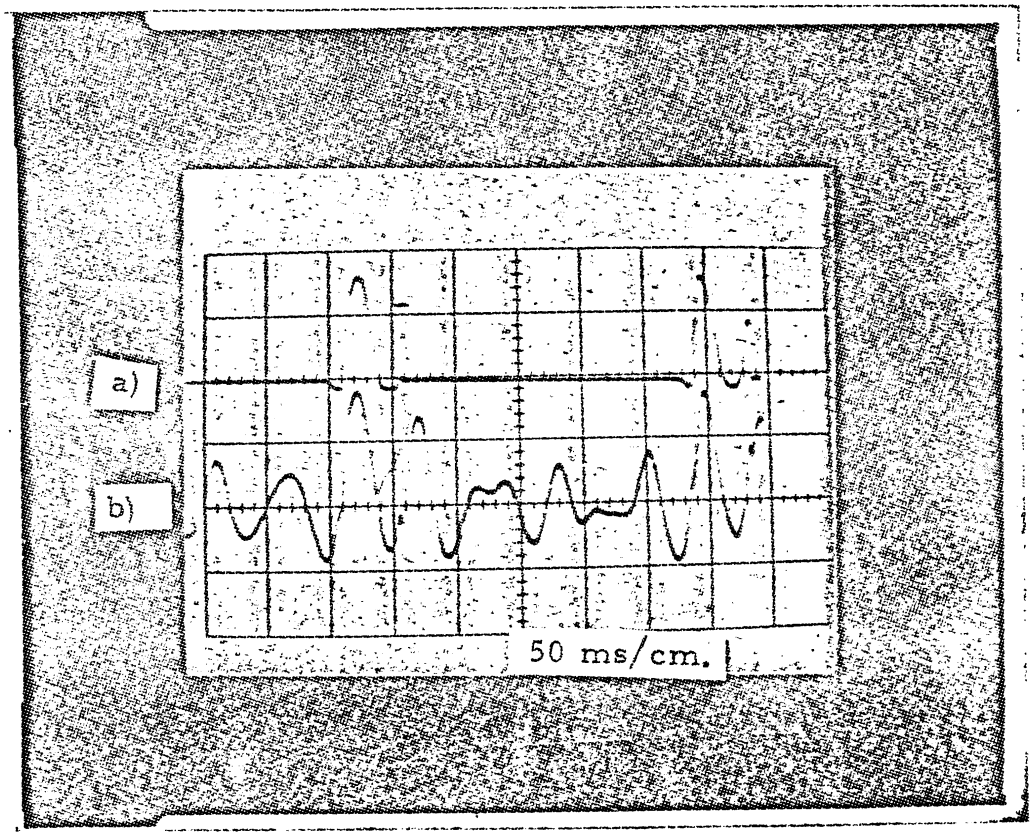


Figure 16 - Oscilloscope Output from U-M Probe in Venturi (a.) with and b.) without Pulse - Shaper).